

# Chain flow in thermo-stimulated creep experiments: application to poly(methyl methacrylate)

A. Dufresne\*, S. Etienne† and J. Perez

*Groupe d'Etudes de Métallurgie Physique et de Physique des Matériaux, URA CNRS 341, Institut National des Sciences Appliquées de Lyon, 69621 Villeurbanne cedex, France*

and P. Demont, M. Diffalah, C. Lacabanne and J. J. Martinez

*Laboratoire de Physique des Solides, URA CNRS 74, Université Paul Sabatier, 31062 Toulouse cedex, France*

(Received 8 June 1994; revised 11 July 1995)

Experimental data from thermo-stimulated creep (TSCr) spectrometry display a retardation mode in poly(methyl methacrylate) (PMMA) at  $T > T_g$  (glass transition temperature). In this work an attempt is made to relate the restoring force involved during TSCr measurements beyond the glass transition zone to the viscoelastic behaviour of the polymeric chains flowing in the entangled network. In order to determine the temperature dependence of the molecular relaxation time, or lifetime for monomer diffusion,  $\tau_{mol}$ , three different sources of viscoelastic measurements are used. The TSCr data are then mapped onto the Arrhenius diagram of  $\log \tau_{mol}$  to deduce the corresponding terminal relaxation time, or flow time,  $\tau_{flow}$ . Comparison between the terminal relaxation time and the characteristic time of TSCr spectrometry shows that, during the temperature scan, the recovery of the frozen-in strain can be effectively well described by the long-range diffusion of macromolecular chains within the surrounding entanglement lattice. Copyright © 1996 Elsevier Science Ltd.

(Keywords: chain flow; thermo-stimulated creep; poly(methyl methacrylate))

## INTRODUCTION

At  $T > T_g$ , i.e. in the rubbery state, the behaviour of the material is mainly explained in terms of entropic elasticity. Beyond a critical length, chains are entangled. The viscoelastic properties of entangled macromolecules are well described by assuming they relax by diffusion along their own contours among topological obstacles coming from neighbouring chains. This process was introduced in terms of reptation by de Gennes<sup>1</sup> and developed by Doi and Edwards<sup>2,3</sup>.

Three viscoelastic behaviour regions can be distinguished at  $T > T_g$  for high molecular weight polymers from the real and imaginary parts of the dynamic shear modulus,  $G'$  and  $G''$ , respectively, when measured as a function of frequency (see *Figure 1*).

(i) At the lowest frequencies, the plots  $\log G'$  ( $\log \omega$ ) and  $\log G''$  ( $\log \omega$ ) exhibit positive slopes for which values are +2 and +1, respectively. The viscoelastic properties in this 'terminal' zone are dominated by parameters such as zero-shear viscosity  $\eta_0$ , steady-state

compliance  $J_e^0$  and terminal relaxation time  $\tau_{flow}$ . After an observation time  $t_{exp} > \tau_{flow}$ , the properties of the system depend on the fluctuations of the entanglements lattice: hence  $\tau_{flow}$  is the relaxation time due to the loss of entanglements of chains ( $\tau_{flow} = \eta_0 J_e^0$ ). For linear polymers, experimental data on the molecular weight dependence of  $\eta_0$  or  $\tau_{flow}$  generally support the power law  $\eta_0 \propto M^{3.4}$  for systems of narrow distribution samples<sup>4–6</sup>, but results differ for widely polydisperse samples. This is valid beyond a critical length which varies according to chain flexibility and dimension (radius of gyration)<sup>7</sup>. Below this critical length, the viscosity appears to be proportional to the chain length<sup>8</sup>.

This change of regime in the viscosity variations is explained by an entanglement concept, that is strong interactions between chains, which originate beyond a critical molecular length<sup>8</sup>. The first model taking into account the existence of entanglements was suggested in 1952 by Bueche; this model predicts a  $\eta_0 \propto M^{3.5}$  law<sup>9,10</sup>. The non-Newtonian flow theory proposed by Graessley<sup>11,12</sup> predicts a similar variation ( $\eta_0 \propto M^{3.5}$ ). The Eyring theory suggests a  $\eta_0 \propto M^{3.33}$  variation from a three-dimensional diffusion model<sup>13</sup>. De Gennes proposed a chain reptation model involving a terminal relaxation time or viscosity ( $\eta_0 \propto M^{3.0}$ ) for which variation is close to that experimentally observed by de Gennes ( $\eta_0 \propto M^{3.3}$ ) (ref. 1).

\*Present address: Centre de Recherches sur les Macromolécules Végétales, CERMAV/CNRS, BP 53, 38041 Grenoble cedex 9, France; and to whom correspondence should be addressed

†Present address: Laboratoire de Métallurgie Physique et Science des Matériaux, URA CNRS 155, Ecole des Mines de Nancy, Parc de Saurupt, 54042 Nancy cedex, France

(ii) At the highest frequencies, all the curves  $\log G'(\log \omega)$  (and also  $\log G''(\log \omega)$ ) tend to merge, whatever the molecular weight may be, for a given polymer (transition region from the rubbery liquid to the glassy state). This transition zone constitutes the main or primary  $\alpha$  relaxation associated with the glass transition. The rheological behaviour in this frequency range is well predicted, from a physical basis, assuming concepts such as hierarchical correlation, density fluctuation sites or quasi-point defects and shear-microdomain nucleation<sup>14,15</sup>.

(iii) Between these two relaxation regions, the curves reach a plateau zone where  $G'(\omega)$  weakly increases with frequency and roughly takes a constant value ( $G'(\omega) \sim G'_e(0)$ ). This plateau zone, for which the length

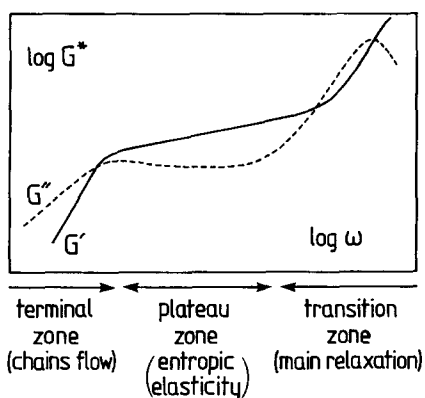


**Figure 1** Schematic variations of  $\log G'$  (—) and  $\log G''$  (---) versus  $\log \omega$  in the low-frequency range

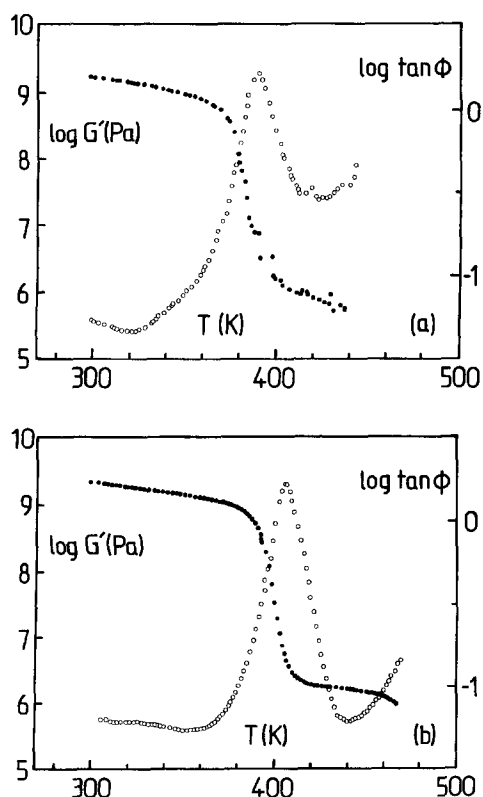


**Figure 2** Variation of  $\log G'$  (●) and  $\log \tan \phi$  (○) measured for a fixed frequency of 0.1 Hz and plotted versus temperature: (a) PMMA 1; (b) PMMA 3. Heating rate = 1 K min<sup>-1</sup>

**Table 1** Codification and characteristics of the samples

Codification	$T_g$ (K)	$\bar{M}_n$ (g mol <sup>-1</sup> )	$\bar{M}_w$ (g mol <sup>-1</sup> )	$\bar{M}_w/\bar{M}_n$
1	383.2	63 000	120 000	1.90
2	384.3	357 000	1 210 000	3.39
3	385.3	667 000	1 350 000	2.02
4	—	56 000	110 000	1.96
5	—	58 000	98 600	1.70

increases with the molecular weight, is assigned to some entanglement persistence, providing a rubber-like response in that scale of frequencies or times. An illustration of the molecular-weight dependence on the plateau zone length is given in Figure 2. This figure shows the variation of the real part of the dynamic shear modulus  $G'$  and of the mechanical loss tangent  $\phi = G''/G'$  measured for a fixed frequency of 0.1 Hz and plotted against the temperature. These measurements were carried out via a low-frequency inverted forced oscillation pendulum. The two sets of data exhibit the behaviour of two different PMMA labelled 1 (Figure 2a) and 3 (Figure 2b) that will be described in the 'Experimental' section. PMMA 1 is characterized by a low molecular weight, whereas PMMA 3 is distinguished by a high molecular weight. Beyond the main or  $\alpha$  relaxation the mechanical loss tangent exhibits an increase, which is connected with macromolecular chain flow. The higher the molecular weight, the higher is the temperature of  $\tan \phi$  increase.

According to the snake-like or reptation concept introduced by de Gennes<sup>1</sup>, the topological constraints due to the fact that the molecules cannot pass through each other confine each chain inside a tube-like region. Hence, physically, the terminal relaxation time  $\tau_{\text{flow}}$  is essentially the time required for complete renewal of the tube. It is the longest time observed in mechanical measurements. To eliminate its original tube, the chain must progress by tube diffusion over a length comparable with its overall length. The corresponding time  $\tau_{\text{flow}}$ , also called reptation time  $\tau_{\text{rep}}$ , or flow time, is expected to follow the experimental scaling form<sup>1</sup>:

$$\tau_{\text{flow}} = \tau_{\text{mol}} N^{3.3} \quad (1)$$

where  $\tau_{\text{mol}}$  is the molecular mobility relaxation time, which is characteristic of the lifetime for the movement of a structural unit, i.e. a monomer unit, over a distance comparable to its size, and  $N$  is the number of repeat units in one chain, also called the degree of polymerization or polymerization number. It should be noted that  $\tau_{\text{mol}}$  is the key to the time-dependent responses and the kinetic transition from the rubbery liquid to the glassy state<sup>14,15</sup>.

In this paper, the viscoelastic properties of poly(methyl methacrylate) (PMMA) of various molecular weights above the glass transition temperature are evaluated using thermo-stimulated creep (TSCr) spectrometry. The aim of this work is to relate the rules governing the polymeric chain flow phenomena at the end of the rubbery plateau to those concerning the TSCr experiments in the vicinity of the high retardation mode (beyond the  $\alpha$  relaxation region). In this way an attempt will be made to compare the value of the following ratios:

$$(i) \frac{\tau_{\text{flow}}}{\tau_{\text{mol}}} (= N^{3.3}) \quad \text{and} \quad (ii) \frac{\tau_{\text{TSCr}}}{\tau_{\text{mol}}(T_{\alpha 1})}$$

where  $\tau_{\text{TSCr}}$  represents the characteristic time of the TSCr experiment and  $\tau_{\text{mol}}(T_{\alpha 1})$  the molecular mobility relaxation time deduced from mechanical spectroscopy and extrapolated to the temperature  $T_{\alpha 1}$  (temperature position of the high-temperature retardation mode, which in the present study will be labelled  $\alpha_1$ ).

## EXPERIMENTAL

### Materials

Different samples of atactic poly(methyl methacrylate) (PMMA) for which codifications are presented in Table 1 were chosen for this study. The corresponding mean features, i.e. glass transition temperature, number-average molecular weight  $\bar{M}_n$  and weight-average molecular weight  $\bar{M}_w$ , together with polymolecularity index ( $\bar{M}_w/\bar{M}_n$ ), are also listed in Table 1. PMMA 1 and PMMA 4 were provided by Norsolor, France. PMMA 1 was copolymerized with 4% ethylene acrylate as comonomer to ensure good thermal stability, while PMMA 4 was copolymerized with 1.5% ethylene acrylate. PMMA 2 was obtained from Röhm and Haas Co., Germany, and PMMA 3 was purchased from Goodfellow Co., Great Britain. PMMA 5 was prepared by the Thermodynamic and Physical Chemistry Laboratory, Valencia Polytechnic University, Spain.

Gel permeation chromatography (g.p.c.) was used to yield  $\bar{M}_w$  and  $\bar{M}_n$ . The calorimetric glass transition temperatures  $T_g$  were found using a Perkin-Elmer DSC-7<sup>16</sup>. The  $T_g$  was assigned to the temperature position of the inflection point. In all d.s.c. experiments, the heating rate was  $20 \text{ K min}^{-1}$ .

### Viscoelastic measurements

Three different sources of viscoelastic measurements have been used<sup>17-19</sup> in order to determine the temperature dependence of the molecular mobility relaxation time  $\tau_{\text{mol}}$ .

- (i) Dynamic modulus measurements<sup>17,18</sup> were carried out with a low-frequency inverted forced oscillation pendulum described elsewhere<sup>20</sup>. The real and imaginary parts of the shear modulus,  $G'$  and  $G''$  respectively, and  $\tan \phi = G''/G'$  can be measured as a function of frequency between  $10^{-5}$  and 1 Hz for different temperatures or versus temperature at a given frequency. This study was performed using PMMA 4 and 5.
- (ii) From ref. 19 two instruments were used to determine properly the viscoelastic properties over an extended temperature range covering the glass transition region, the rubbery plateau and the terminal zone. The glass transition region was explored using a hydraulic testing machine (MTS 831-10) operated in the tensile mode. Twelve driving frequencies per decade were chosen in the range 0.01–40 Hz. Both the rubbery plateau and terminal zones were investigated by oscillatory shear measurements performed on a Weissenberg-type rheometer (Rheometrics RMS 605) operated with a parallel-disc geometry. The range of driving frequencies was 0.0016–0.016 Hz. This study was performed using PMMA 4.
- (iii) Additional data in the rubbery state were obtained from thermo-stimulated creep (TSCr) spectrometry.

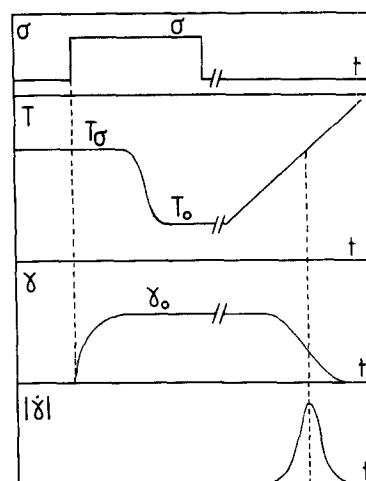


Figure 3 Thermo-stimulated creep spectrometry principle

This study was performed using different molecular weight materials, i.e. PMMA 1, 2 and 3<sup>16</sup>. During the past 16 years, TSCr spectrometry has been used successfully to study molecular mobility in polymers by Lacabanne *et al.*<sup>21-27</sup>. The principle of the TSCr technique and the torsion pendulum used for this work have been described elsewhere<sup>21</sup>. A more complete description of the experimental set-up will be found in ref. 22. In brief (see also Figure 3): (a) The sample is subjected to a static mechanical stress  $\sigma$  at a given temperature  $T_\sigma$  for a time ( $\sim 2$  min) allowing complete orientation of the mobile units that one wishes to consider. (b) This out-of-equilibrium configuration (viscoelastic strain  $\leq 10^{-3}$ ) is then frozen by a rapid quench to a temperature  $T_0$  much lower than  $T_\sigma$  where any molecular motion is hindered. The stress is then removed. (c) The release of the frozen-in strain is induced by a controlled increase of the temperature ( $7 \text{ K} \cdot \text{min}^{-1}$ ). The response  $\gamma$ , its time derivative  $\dot{\gamma}$  and the temperature are simultaneously recorded versus time  $t$ .

The plot of the normalized magnitude,  $|\dot{\gamma}/\sigma|$ , against temperature represents the complex TSCr spectrum. Phenomenologically, the recovery behaviour can be described by a Kelvin-Voigt model. The mechanical retardation time  $\tau$  can be deduced from measurements of  $\dot{\gamma}(T)$  and  $\gamma(T)$ :

$$\tau(T) = \left| \frac{\gamma(T)}{\dot{\gamma}(T)} \right| \quad (2)$$

Not only does this technique permit the measurement and the characterization of the anelastic effect associated with the glass transition, but its low equivalent frequency (about  $10^{-3}$  Hz) allows the resolution of overlapping energy-loss peaks, frequently met in broad retardation modes. In polymers, and more generally in disordered systems, the model of a single retardation time must be generalized in order to obtain a good fit between theory and experiment; this is generally done by using a distribution of retardation times. The great advantage of the TSCr technique is that it allows a detailed study of this distribution.

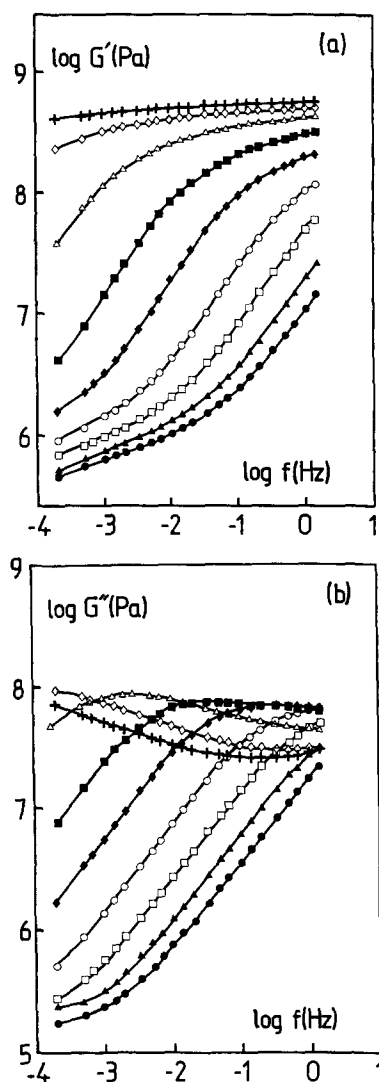


**Figure 4** Isothermal curves of (a) storage modulus  $G'(\omega)$  and (b) loss modulus  $G''(\omega)$  versus  $\log$ [frequency (Hz)] for PMMA 4 measured at different temperatures: (+) 380 K; ( $\diamond$ ) 382 K; ( $\Delta$ ) 386 K; ( $\blacksquare$ ) 389 K; ( $\blacklozenge$ ) 392 K; ( $\circ$ ) 395 K; ( $\square$ ) 398 K; ( $\blacktriangle$ ) 401 K; ( $\bullet$ ) 403 K

## RESULTS

### Dynamic mechanical analysis

It is obvious that the Williams–Landel–Ferry (WLF) equation, based on the free-volume concept, provides a reasonably good description of the viscoelastic behaviour in the high-temperature region, but is not quite valid as temperature decreases near  $T_g$ . In this last temperature range a molecular kinetic theory has been proposed on a physical basis<sup>14,15</sup>. Nevertheless, we will first present viscoelastic measurements performed on PMMA and analysed using the classical WLF shift factor<sup>28</sup>. From these experimental data we will then interpolate the various results to build up the temperature dependence of the lifetime  $\tau_{\text{mol}}$  for monomer diffusion.

In Figures 4a and 4b, the values of  $G'$  and  $G''$  are plotted against frequencies for PMMA 4 between  $10^{-4}$  and 1 Hz at different temperatures from ref. 17. Then, as is usually done in such studies<sup>29</sup> and according to the time–temperature superposition principle, an attempt was made to superimpose the curves by simply shifting them along the frequency scale to produce a master curve

over an enlarged range of frequencies at the reference temperature  $T_0$ . In principle, a vertical shift  $\rho T/\rho_0 T_0$  should also be applied to account for the change in polymer density  $\rho - \rho_0$  between  $T$  and  $T_0$ . Actually, this correction is very small on the restricted temperature range under consideration and vertical shifts are neglected. The reliability of shifting  $G'$  and  $G''$  curves was established by the use of the same shift factor for both data.

In the  $\alpha$  relaxation region (but above  $T_g$ ), the temperature dependence of the horizontal shift factor  $a_T$  is expected to obey the well known WLF equation<sup>29</sup>:

$$\log a_T = \log\left(\frac{f_0}{f}\right) = \log\left(\frac{\tau_{\text{mol0}}}{\tau_{\text{mol}}}\right) = -\frac{C_1^{T_0}(T - T_0)}{C_2^{T_0} + (T - T_0)} \quad (3)$$

where  $f_0$  and  $f$  are the frequencies of the motions at temperatures  $T_0$  and  $T$ , respectively,  $\tau_{\text{mol0}}$  and  $\tau_{\text{mol}}$  the corresponding molecular mobility relaxation times defined as the inverse of the frequency of the maximum in  $G''$ ,  $(2\pi f)^{-1}$  and  $(2\pi f_0)^{-1}$  respectively, and  $C_1^{T_0}$  and  $C_2^{T_0}$  are the values of the viscoelastic coefficients at the reference temperature  $T_0$ . It is usual to consider as the reference temperature the quantity  $T_\alpha(1 \text{ Hz})$ , defined as the temperature at which  $G''$  goes through a maximum when the frequency is 1 Hz. The corresponding temperature is  $T_\alpha(1 \text{ Hz}) = T_0 = 395 \text{ K}$  in our case. According to equation (3),  $C_1^{T_0}$  and  $C_2^{T_0}$  can be conveniently derived from plots of  $(T - T_0)/\log a_T$  versus  $(T - T_0)$ . The values of the viscoelastic coefficients can be derived from the slope and intercept with the y axis of this straight line. Thus the coefficients so deduced are reported in Table 2. Data with  $|T - T_0| < 5^\circ\text{C}$  were neglected because of large uncertainties in the quantity  $(T - T_0)/\log a_T$ .

PMMA 5 has been studied using the same inverted forced oscillation pendulum<sup>18</sup>. Taking as reference temperature  $T_0 = 385 \text{ K}$ , the following coefficients were obtained:  $C_1^{385} = 11.3$ ,  $C_2^{385} = 28.3^\circ\text{C}$ . With a view to obtaining a single relaxation time scale, values of the coefficients should be determined systematically at the temperature  $T_\alpha(1 \text{ Hz}) = 395 \text{ K}$ , taken as the reference temperature. This is achieved using:

$$C_1^{T_0} C_2^{T_0} = C_1^{395} C_2^{395} \quad (4)$$

$$395 - C_2^{395} = T_0 - C_2^{T_0} = T_\infty \quad (5)$$

where  $C_1^{395}$  and  $C_2^{395}$  denote the values of the viscoelastic coefficients at  $T_\alpha(1 \text{ Hz})$ . Assuming WLF equation validity at low temperature,  $T_\infty$  as defined in equation (5) is the temperature at which the cooperative motions involved in the glass transition would appear at infinitely low driving frequency. It corresponds to an infinite value of the horizontal shift factor  $a_T$ . Using equations (4) and (5) for PMMA 5 the coefficients reported in Table 2 and corresponding to ref. 18 are obtained.

PMMA 4 was also studied over an extended temperature range<sup>19</sup>. Viscoelastic properties were determined

**Table 2** Experimental and interpolated viscoelastic coefficients

Source	17	18	19	Interpolation
$C_1^{395}$	7.1	8.3	9.8	11
$C_2^{395}$ ( $^\circ\text{C}$ )	32.7	38.3	32.5	40

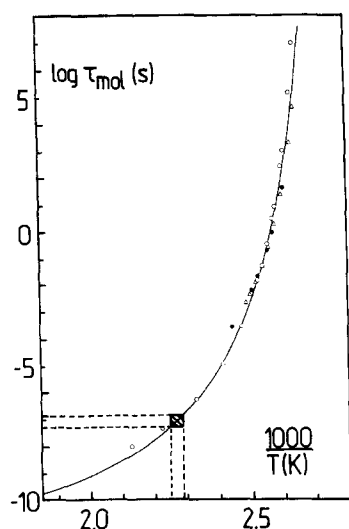


**Figure 5** Temperature dependence of the molecular mobility relaxation time  $\tau_{\text{mol}}$  in an Arrhenius plot: ( $\Delta$ ) experimental data from ref. 17; ( $\bullet$ ) experimental data from ref. 18; ( $\circ$ ) experimental data from ref. 19; (—) interpolated curve. The hatched zone indicates the temperature position range of the  $\alpha_1$  TSCr peak for PMMA 1

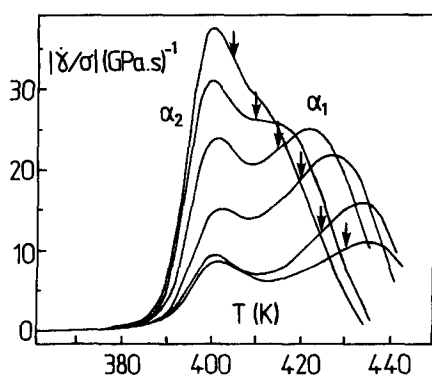


**Figure 6** Thermo-stimulated creep (TSCr) spectra in PMMA 1. The stress is applied for 2 min at various temperatures  $T_\sigma$ , indicated by a small arrow

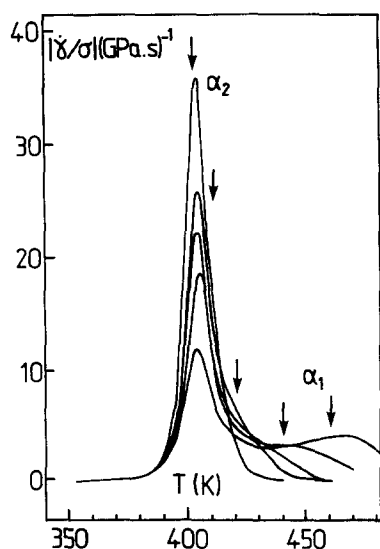


**Figure 7** Thermo-stimulated creep (TSCr) spectra in PMMA 2. The stress is applied for 2 min at various temperatures  $T_\sigma$ , indicated by a small arrow

using two instruments in the temperature range 380–398 K and 405–470 K as previously quoted. Taking as reference temperature  $T_0 = 398$  K, the following values of  $C_1^{398}$  and  $C_2^{398}$  were reported:  $C_1^{398} = 9.0$ ,  $C_2^{398} = 35.5^\circ\text{C}$ . With  $T_{\alpha}(1\text{ Hz}) = 395$  K as the reference temperature, the values reported in Table 2 from ref. 19 are obtained.

From the frequency position of isothermal  $G''$  curves (Figure 4b) the following relation can be deduced between  $\tau_{\text{mol}}$ ,  $C_1^{395}$  and  $C_2^{395}$ :

$$\log[\tau_{\text{mol}}(\text{s})] = -1.2 - \frac{C_1^{395}(T - 395)}{C_2^{395} + (T - 395)} \quad (6)$$

This relation allows us to build up the temperature dependence of  $\log \tau_{\text{mol}}$  in an Arrhenius diagram (Figure 5). This plot exhibits a strong variation with temperature typical of the primary glass–rubber relaxation. Experimental data from different sources align more or less properly on a single curve. Accordingly, we have fitted the  $\log \tau_{\text{mol}}$  values via a WLF-like equation to obtain the best interpolated curve on the whole temperature range (full line on Figure 5). From trial and error upon the various data the best fit is obtained with the following general coefficients (also listed in Table 2):  $C_1^{395} = 11$ ,  $C_2^{395} = 40^\circ\text{C}$ .

It is noteworthy that the WLF equation is unable to describe accurately the viscoelastic behaviour of the polymer over the whole temperature range. Similarly, Murthy<sup>30,31</sup> and Perez *et al.*<sup>32</sup> have shown that equation (3) or its equivalent, the Vogel–Fulcher–Tamman (VFT) equation, failed to describe the experimental data over a wide temperature range. But it must be emphasized that only the most valuable figure for  $\tau_{\text{mol}}$  extrapolated towards the temperature range around  $T_{\alpha 1}$  is required in the present study.

This interpolated curve will be used subsequently to infer lifetimes for monomer movements  $\tau_{\text{mol}}(T_{\alpha 1})$  from thermo-stimulated creep measurements. Indeed, the experimental determination of the temperature position of the high-temperature TSCr retardation mode ( $T_{\alpha 1}$ ) allows one to deduce the  $\tau_{\text{mol}}(T_{\alpha 1})$  value directly from Figure 5.

#### Thermo-stimulated creep (TSCr) analysis

TSCr analysis has been performed to characterize the anelastic properties above the glass transition for the three PMMA samples: 1, 2 and 3<sup>17</sup>. Before any temperature scan, the sample was first heated at  $T_g + 20^\circ\text{C}$  free from any applied stress for 30 min. This thermal processing removes the thermal history and the effects of physical ageing and residual internal stresses.

Figures 6 to 8 show the complex TSCr spectra obtained for PMMA 1, 2 and 3 respectively. A static shear stress  $\sigma$  ( $= 0.27$  MPa for PMMA 1,  $0.47$  MPa for PMMA 2 and  $0.75$  MPa for PMMA 3) was applied at a temperature  $T_\sigma$  as indicated by arrows for 2 min. The resulting viscoelastic strain was then frozen by quenching the sample to  $T_\alpha - 100$  K. The variation of  $\dot{\gamma}$  was normalized to the applied stress. So, even though different stresses were applied to the three polymers, a comparative study is possible. Examination was also made for non-linear effects, which were negligible. The term ‘complex’ is used as opposed to elementary TSCr spectrum involving the ‘fractional stresses’

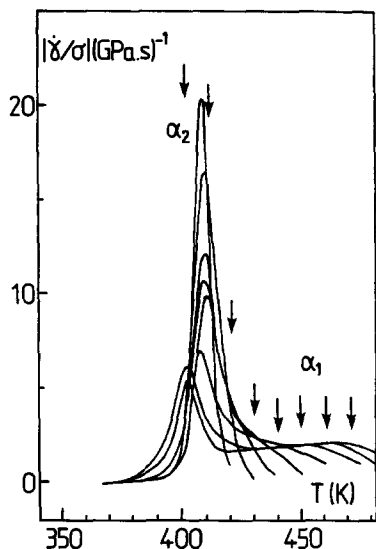


**Figure 8** Thermo-stimulated creep (TSCr) spectra in PMMA 3. The stress is applied for 2 min at various temperatures  $T_\sigma$ , indicated by a small arrow

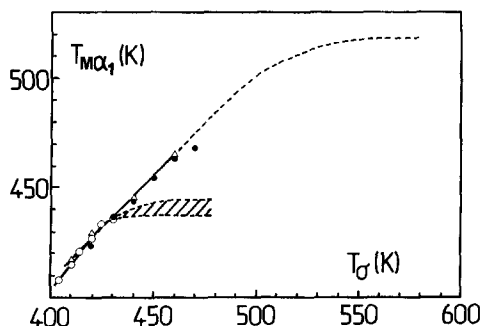


**Figure 9** Evolution of the temperature position of the  $\alpha_1$  retardation mode versus stress application temperature: (○) PMMA 1; (△) PMMA 2; (●) PMMA 3

technique<sup>21–25,27</sup>. The same stress  $\sigma$  was applied to the sample at different temperatures ( $T_\sigma$  as indicated by small arrows on spectra).

From Figures 6 to 8 two retardation modes labelled  $\alpha_1$  and  $\alpha_2$  as temperature decreases are resolved. The  $\alpha_2$  mode appears near the glass transition zone, which was determined by d.s.c.<sup>16</sup>. Consequently, it has been assigned to the anelastic manifestation of the main  $\alpha$  relaxation of PMMA. This mechanism involves cooperative motions of long chain sequences. It will not be discussed hereafter.

Contrary to the  $\alpha_2$  mode, the temperature position of the  $\alpha_1$  peak (when detectable on the TSCr spectra) depends on the conditions of stress application. As the temperature  $T_\sigma$  of stress application increases, the  $\alpha_1$  mode appears progressively, at first as a shoulder, and then as a resolved peak, which shifts towards higher temperatures with increasing  $T_\sigma$  values. Figure 9 displays the evolution of the temperature position of the TSCr  $\alpha_1$  peak,  $T_{M\alpha_1}$ , versus the temperature of stress application,  $T_\sigma$ , for the three materials. This temperature  $T_\sigma$  was increased until the experimental limiting value<sup>16</sup>. At higher temperature, irrecoverable creep or viscous polymer flow involving sudden fall of the stiffness of the specimen and the end of the rubbery plateau occur.

Indeed, in this temperature range, we are approaching the experimental limit of TSCr spectrometry. Although not shown by experimental data, the evolution of  $T_{M\alpha_1}$  towards high temperatures indicates that the 'true' position, labelled  $T_{\alpha_1}$ , of the  $\alpha_1$  mode is higher. It is impossible to reach it experimentally, but it can be obtained by extrapolation (Figure 9). Such limiting temperature depends on the molecular weight of the polymer. It is difficult to assign a definite value of  $T_{\alpha_1}$  for each material tested in the TSCr experiment, particularly in the case of PMMA 2 and 3, for which  $T_{\alpha_1}$  seems to be much higher than the last experimental point.

For PMMA 1 we prefer to associate a  $T_{\alpha_1}$  temperature range, rather than a definite value. We cannot hope for more than a tendency, despite the fact that the determination of the 'true' temperature  $T_{\alpha_1}$  at which the unattributed  $\alpha_1$  retardation mode occurs is the key point. Such an extrapolation shows that  $T_{M\alpha_1}$  stabilizes around 437–445 K for PMMA 1. As expected in view of relaxation, the high-temperature retardation mode seems to shift to higher temperature as the molecular weight increases.

## DISCUSSION

This limiting temperature range for PMMA 1 can then be used to calculate the molecular mobility relaxation time  $\tau_{mol}$  at  $T_{\alpha_1}$  from the extrapolated WLF type of equation fitted to the experimental damping data. The  $\tau_{mol}$  range in question is indicated by the hatched zone on the interpolate curve of Figure 5. The corresponding relaxation times are estimated between  $\tau_{mol}(T_{\alpha_1}) = 1.5 \times 10^{-7}$  s and  $4.9 \times 10^{-8}$  s. These values can also be deduced from equation (6). The flow time, or terminal relaxation time,  $\tau_{flow}$  can then be calculated based on equation (1). The number  $N$  of repeat units in one chain was evaluated from g.p.c. measurements of  $\bar{M}_n$ , divided by the molar mass of PMMA equal to  $100 \text{ g mol}^{-1}$ . The corresponding results are  $\tau_{flow} = 2.6 \times 10^2$  s and  $8.5 \times 10^1$  s. These flow times will then be compared with the TSCr characteristic time.

It is worthwhile to note that in thermo-stimulated experiments, i.e. thermo-stimulated creep (TSCr) or currents (TSC) techniques, the complex spectrum generally exhibits a more or less broad peak at  $T > T_g$ , depending upon the complexity of molecular relaxation processes occurring in the studied temperature–time range. But TSC exhibits a different behaviour for PMMA since its super- $T_g$  relaxation mode is found at significantly lower temperature than in TSCr. Indeed the TSC spectrum is constituted by a broad peak around 423 K. This result can be explained by a molecular mobility between entanglements and has been attributed to the dielectric manifestation of the 'liquid–liquid transition'<sup>33</sup>. The existence of a so-called 'liquid–liquid transition' labelled  $T_{ll}$  in polystyrene above the glass transition  $T_g$  was first proposed by Boyer in 1963<sup>34</sup>. Since that time many other reports of observation of a transition above  $T_g$  have been carried out in numerous polymers. Nevertheless, the phenomenon described here (i.e. in TSCr experiments) exhibits different features (mainly the molecular-weight dependence).

It is quite different in TSCr analysis during the recovery of the strain. This paper is an attempt to interpret the result obtained by TSCr spectrometry. If

we assume that at  $T > T_g$  the restoring force involved in the TSCr experiment could be related to the viscoelastic behaviour of the polymeric chains flowing in the network of entanglements, so the relaxation time at  $T_{\alpha_1}$  should be equal to  $\tau_{\text{flow}}(T_{\alpha_1})$ . According to the equivalent frequency of the TSCr technique ( $10^{-3}$  Hz)<sup>21,23,25</sup>, the characteristic time  $\tau_{\text{TSCr}}$  in TSCr measurements is about  $1.6 \times 10^2$  s. The value of the equivalent frequency was established by comparing the mechanical loss compliance  $J''$  worked out from elementary processes as a function of temperature and frequency to the TSCr spectrum for the used heating rate.

A perfect agreement is observed between flow time and TSCr characteristic time for PMMA 1 (260–85 s and 160 s respectively). For this material, the restoring force involved during the  $\alpha_1$  TSCr retardation mode recording can be undoubtedly related to the long-range diffusion of polymeric chains. So, it should conceivably also be the case for PMMA 2 and 3, for which the  $T_{\alpha_1}$  values were dubious. We can try to invert the problem and to consider that the  $\tau_{\text{flow}}$  value is equivalent to  $\tau_{\text{TSCr}}$ , and then to proceed towards the  $T_{\alpha_1}$  limiting temperature. This process can then be validated if this temperature agrees with the experimental points. Starting from  $\tau_{\text{TSCr}} = \tau_{\text{flow}} = 160$  s, it gives, using equation (1),  $\tau_{\text{mol}} = 3.0 \times 10^{-10}$  s and  $\tau_{\text{mol}} = 3.8 \times 10^{-11}$  s for PMMA 2 and 3 respectively. The corresponding  $T_{\alpha_1}$  temperatures obtained via equation (6) or Figure 5 are 519 K and 602 K respectively. For PMMA 2, this value seems to be reasonable as displayed by the dotted line on Figure 9, or at least we can conclude that  $\tau_{\text{TSCr}}$  and  $\tau_{\text{flow}}$  are of the same order of magnitude. On the other hand, it is quite different for PMMA 3, and we observe a discrepancy between the  $T_{\alpha_1}$  value (602 K) and experimental values on Figure 9. This situation becomes clear on thinking it over in the light of the g.p.c. results. Indeed, the g.p.c. curve for PMMA 3 exhibits a significant tail on the low-molecular-weight side. So we can conclude that these low-molecular-weight chains are responsible for the  $\alpha_1$  retardation mode. It must also be pointed out that these last two materials (PMMA 2 and 3) exhibit a broader molecular-weight distribution as displayed in Table 1 and from the aspect of the  $\alpha_1$  retardation mode on Figures 7 and 8. Indeed, it is shown that the experimental power law (equation (1)) is roughly valid for very close polydispersities, except for high molecular weights, and a decrease of viscosity with polydispersity is also predicted<sup>35</sup>. This can be a possible explanation of the discrepancy observed for PMMA 3 and possibly to a certain extent for PMMA 2. Moreover, numerous parameters are involved to deduce the flow time from TSCr measurements. In particular, the 'true' temperature of the maximum of the high-temperature peak,  $T_{\alpha_1}$ , is found by means of an extrapolation. It is obvious that this process is more or less accurate. Despite this fact, very satisfactory agreement in the order of magnitude is displayed between  $\tau_{\text{flow}}$  and the TSCr characteristic time. A perfect agreement is observed for polymers with low molecular weight and close polydispersity and this agreement shades off progressively for higher polydispersities and higher molecular weights.

## CONCLUSION

This study shows that the restoring force involved in thermo-stimulated creep (TSCr) measurements beyond the glass transition region can be clearly related to the viscoelastic behaviour of polymeric chains flowing by diffusion within the surrounding entangled network. During the temperature scan, the recovery of the previously frozen-in strain can be well described by the chain diffusion concept. It explains the difference in thermo-stimulated current and creep behaviours in this temperature range, since the former technique does not involve flow. It was carried out on poly(methyl methacrylate) but could be extended to any amorphous entangled polymer.

## REFERENCES

- 1 de Gennes, P.-G. *J. Chem. Phys.* 1971, **55**, 572
- 2 Doi, M. and Edwards, S. F. *J. Chem. Soc., Faraday Trans (II)* 1978, **74**, 1789, 1802, 1818
- 3 Doi, M. and Edwards, S. F. *J. Chem. Soc., Faraday Trans. (II)* 1979, **75**, 38
- 4 Montfort, J. P., Marin, G., Arman, J. and Monge, Ph. *Polymer* 1978, **19**, 277
- 5 Prest, M. W. and Porter, R. S. *Polym. J. (Tokyo)* 1973, **4**, 154
- 6 Masuda, T., Kitagawa, K., Inoue, T. and Onogi, S. *Macromolecules* 1970, **3**, 116
- 7 Berry, G. C. and Fox, T. G. *Adv. Polym. Sci.* 1968, **5**, 261
- 8 Graessley, W. W. *Adv. Polym. Sci.* 1974, **16**, 1
- 9 Bueche, F. *J. Chem. Phys.* 1952, **20**, 1959
- 10 Bueche, F. *J. Chem. Phys.* 1956, **25**, 599
- 11 Graessley, W. W. *J. Chem. Phys.* 1965, **43**, 2696
- 12 Graessley, W. W. *J. Chem. Phys.* 1967, **47**, 1942
- 13 Eyring, H., Ree, T. and Hirai, N. *Proc. Natl. Acad. Sci.* 1953, **44**, 1213
- 14 Perez, J., Cavaille, J. Y., Etienne, S. and Jourdan, C. *Rev. Phys. Appl.* 1988, **23**, 125
- 15 Cavaille, J. Y., Perez, J. and Johari, G. P. *Phys. Rev. (B)* 1989, **39**, 2411
- 16 Diffalah, M. PhD Thesis, Toulouse, France, 1993
- 17 Muzeau, E. PhD Thesis, INSA Lyon, France, 1992
- 18 Ouali, N., Mangion, M. B. M. and Perez, J. *Phil. Mag. (A)* 1993, **67** (4), 827
- 19 Halary, J. L., Oultache, A. K., Louyot, J. F., Jasse, B., Sarraf, T. and Muller, R. *J. Polym. Sci. (B) Polym. Phys.* 1991, **29**, 933
- 20 Etienne, S., Cavaille, J. Y., Perez, J., Point, R. and Salvia, M. *Rev. Sci. Instrum.* 1982, **53**, 1261
- 21 Monpagens, J. C., Chatain, D., Lacabanne, C. and Gautier, P. *J. Polym. Sci. (B) Polym. Phys.* 1977, **15**, 767
- 22 Stefanel, M. PhD Thesis, Toulouse, France, 1984
- 23 Lacabanne, C., Chatain, D., Monpagens, J. C. and Berticat, P. *J. Appl. Phys.* 1979, **50**, 2723
- 24 Demont, P., Chatain, D., Lacabanne, C., Ronarc'h, D. and Moura, J. L. *Polym. Eng. Sci.* 1984, **24**, 127
- 25 Demont, P., Fourmaud, L., Chatain, D. and Lacabanne, C. *Adv. Chem. Ser.* 1990, **227**, 191
- 26 Boye, J., Martinez, J. J., Lacabanne, C., Perret, P., Chabert, B. and Gerard, J. F. *Polymer* 1992, **33**, 323
- 27 Dufresne, A. and Lacabanne, C. *Polymer* 1993, **34**, 3173
- 28 Williams, M. L., Landel, R. F. and Ferry, J. D. *J. Am. Chem. Soc.* 1955, **77**, 3701
- 29 Ferry, J. D., 'Viscoelastic Properties of Polymers', 3rd Edn., Wiley, New York, 1980
- 30 Murthy, S. S. N. *J. Polym. Sci. (C) Polym. Lett.* 1988, **26**, 361
- 31 Murthy, S. S. N. *J. Polym. Sci. (B) Polym. Phys.* 1993, **31**, 475
- 32 Perez, J. and Cavaille, J. Y. *J. Non-Cryst. Solids* 1995, **1028**, 172
- 33 Gouari, A., Bendaoud, M., Lacabanne, C. and Boyer, R. F. *J. Polym. Sci. (B) Polym. Phys.* 1985, **23**, 889
- 34 Boyer, R. F. *Rubber Chem. Technol.* 1963, **36**, 1301
- 35 Montfort, J. P., Marin, G. and Monge, Ph. *Macromolecules* 1986, **19**, 1979